Environmental and Earth Sciences Research Journal
Vol. 9, No. 4, December, 2022, pp. 167-173
Journal homepage: http://iieta.org/journals/eesrj

Research on No-bracket Construction of Building Structure Reinforcement

Jiao Li

Department of Civil Engineering, College of Construction Engineering, Jilin University, Changchun 130000, China

Corresponding Author Email: lj17137@outlook.com

https://doi.org/10.18280/eesrj.090406

Received: 10 October 2022
Accepted: 30 November 2022

Keywords:
no-bracket construction, planting-bar technology, pull-out test, finite element simulation

ABSTRACT

This paper studies the no-bracket construction technology for reinforced concrete reinforcement, and uses planting-bar technology as support to solve the problem that the scaffolding cannot be erected for construction due to site factors. Firstly, the steel bar pullout test was carried out to study the influence of concrete strength, planting bar diameter, planting bar depth, and concrete structure type on the pullout force of the planting-bar. Secondly, the finite element method was used to simulate the selection of formwork and planting-bar parameters under different working conditions. The simulation results were basically consistent with the planting-bar pullout test, which provided appropriate formwork parameters and planting-bar parameters for different construction situations and a theoretical reference for the reconstruction and expansion project under the factors such as insufficient site for erection of supports.

1. INTRODUCTION

The reinforcement of concrete structures is generally carried out with the scaffolding method [1-5], in which the wall thickening construction is carried out with the scaffold, which requires a lot of space. However, the uncertainty of the site makes it necessary to find appropriate construction methods and techniques for the reinforcement of concrete structures.

The no-bracket construction technology put forward by a large number of scholars is mainly applied to new reinforced concrete structures, while the research on the reinforcement and reconstruction of existing reinforced concrete structures is relatively shallow. The relatively mature reinforcement methods in concrete structure research include: reinforcement by increasing the cross-sectional area, FRP reinforcement [6-8], carbon fiber sheet reinforcement [9], external pre-stressing reinforcement [10-12], wrapped steel reinforcement [13], external sticking steel plate reinforcement, shotcrete reinforcement technology [14, 15], etc. Among them, the method of increasing the interface area is widely applied for its simple construction technology. It can also ensure the strength of the connection while increasing the structure strength and stiffness. Based on the method of reinforcement by increasing the cross-sectional area, this research proposes a technology of no-bracket reinforcement of reinforced concrete structure with the planting-bar method, which uses the planting-bar reinforcement technology to take the original reinforced concrete structure as the load-bearing structure. In this method, the steel formwork system has fewer supports, which saves the construction cost and solves the problem of insufficient construction site for structural reinforcement.

This paper explores the influence of concrete strength, diameter of the planted-bar reinforcement, planted-bar depth, concrete structure type and other factors on the failure form and ultimate pullout force of planted-bar components by carrying out pullout tests both on the project site and in the laboratory [16-19]. Then, the Abaqus finite element model is established to analyze the stress distribution, bonding state and concrete damage of the planted-bar reinforcement concrete and the reinforcement with planted bar in the process of drawing [20]. The causes of damage in various drawing tests are analyzed, and reasonable suggestions on various parameters of the planted bar are put forward. The lateral force [21-23] of the concrete pouring on the formwork is calculated and the finite element model of the formwork system is set up. In addition, the stress and displacement of relevant components of the steel formwork under different working conditions are analyzed, obtaining the construction parameters for different situations to ensure the construction safety of the formwork.

2. DRAWING TEST OF PLANTED BAR IN CONCRETE STRUCTURE

2.1 Theoretical basis

The no-bracket construction system of reinforced concrete structure consists of three parts: planted-bar bearing system, steel formwork and connection system. The force transfer path is as follows: the concrete pouring load is transferred to the steel formwork first, then the load is transferred to the planted bar bearing system through the connection system, and finally the load is transferred to the original structure by the reinforcement with planted bar.

The strength of planted bars is determined by the bond strength between the adhesive of planted bars and the concrete surface as well as the surface of reinforcement with planted bars. The load transfer path of plain concrete structure is planted-bar reinforcement, planted-bar adhesive [24], and the concrete around the adhesive in turn. This force transfer path also determines that the size of its adhesive force is affected by the fullness of the interface between the adhesive and the

concrete and the reinforcement, concrete strength, planting reinforcement bar depth, and the distance between the planted bars. After the external load of the reinforced concrete structure is transferred to the adhesive, it is transferred to the concrete in the length direction of the planting reinforcement, and then transferred to the built-in reinforcement by the concrete between the planted-bar reinforcement and the built-in reinforcement. Therefore, the spacing of the planting reinforcement has little impact on the strength of the planting reinforcement.

2.2 Test materials and manufacturing

In this test, by controlling the variables, the failure forms and causes of planted –bar reinforcement under the pull out force under different conditions are studied, and the length range of planted reinforcement in reinforcement construction is further analyzed. The test is divided into six groups. See Table 1 and Table 2 for the specific conditions of the test pieces. The pouring size of the plain concrete test specimen is designed to be 350mm × 350mm × 350mm. The reinforced concrete test shall be carried out on the project site, and the spacing between each planting points shall be 200mm. The specific materials are as follows:

(1) Structural materials of test pieces: plain concrete members and reinforced concrete members. The reinforced concrete specimen use the abutment materials at the site of Beijing-Harbin Expressway Project, and its concrete strength is C30 (mix ratio is as follows: cement: medium sand: crushed stone: water=459:542:1206:188). C25, C30 and C35 are selected as the plain concrete test pieces. The mix proportion of C25 and C35 is calculated by referring to the design specification [25], and the same mix proportion of the abutment material test piece is used for C30.

(2) Planted-bar reinforcement: HRB400 is adopted, with 3 diameters (Φ 12, Φ 16 and Φ 20) and 5 planting depths (6d, 8d, 10d, 12d, and 15d).

(3) The planting adhesive used in the test is a modified epoxy adhesive.

2.3 Test plan and results

Number and naming of test piece: the meaning is in order of structure type (RC reinforced concrete, C-plain concrete), concrete strength, diameter of planting bar reinforcement and depth of planted bar. For example, RC-30-16-6 indicates that the test piece is a C30 reinforced concrete test piece, the diameter of the planted bar reinforcement is 16 mm and the depth of the planted bar is 6d.

The specimen is loaded step by step by using a drawing machine, and the loading value increases step by step according to the yield drawing force of the reinforcement, and the increment is one tenth of the yield drawing force. (Taking RC-30-16-6 specimen as an example, the theoretical yield strength of HRB400 reinforcement is 400MPa, the nominal section area of the Φ16 reinforcement is 201.1mm^2, the theoretical yield pullout force of the planted-bar reinforcement is 80.4KN, and the loading increment is 8.04KN. For the convenience of the test, 8 KN is rounded.) If the loading value of the test piece reaches the yield pullout force without damage, loading is kept going on until the test piece is damaged.

See Table 1 and Table 2 for specific values of test results.

The following is obtained through analyzing the data in Table 1 and Table 2:

(1) When the depth of the planted bar is shallow, the ultimate pullout force increases significantly with the increase of concrete strength; when the embedded bars are deep, the increase of concrete strength has little effect on the ultimate pullout force.

(2) The increase of diameter can greatly increase the ultimate pullout force of the specimen, and the greater the depth of the embedded bar is, the greater the influence of the diameter of the embedded bar will be, and the more obvious the increase of the ultimate pullout force becomes.

(3) The ultimate pullout force increases significantly with the increase of planted bar depth: the larger the planted bar diameter is, the greater the pullout force is; However, for concrete specimens with different strength, the ultimate pullout force increases little when increasing the depth of embedded bars.

Table 1. Pulling test data of reinforced concrete specimens

Specimen number	Ultimate drawing force / kN	Average ultimate drawing force / kN
RC-30-12-6	21.5	19.1
	19.2	
	16.7	
RC-30-12-8	26.7	25.4
	25.5	
	24.6	
RC-30-12-10	30.2	30.7
	32.6	
	29.2	
RC-30-12-12	36.4	35.7
	35.6	
	35.2	
RC-30-12-15	42.4	40.8
	40.2	
	39.7	
RC-30-16-6	35.2	34.7
	32.4	
	36.6	
RC-30-16-8	46.2	43.7
	44.4	
	40.4	
RC-30-16-10	54.5	58.7
	59.2	
	62.4	
RC-30-16-12	74.6	77.1
	79.2	
	77.5	
RC-30-16-15	90.1	87.6
	84.4	
	88.3	
RC-30-20-6	55.5	58.8
	61.3	
	59.5	
RC-30-20-8	66.5	71.4
	70.2	
	77.4	
RC-30-20-10	97.2	94.3
	93.4	
	92.2	
RC-30-20-12	112.4	118.1
	119.3	
	122.5	
RC-30-20-15	133.3	135.1
	137.7	
	134.3	

Table 2. Pulling test data of plain concrete specimens

Specimen number	Ultimate drawing force / kN	Average ultimate drawing force / kN
C-25-16-6	26.2	25.7
	25.2	
C-25-16-8	35.0	36.2
	37.3	
C-25-16-10	44.5	46.1
	47.6	
C-25-16-12	70.7	72.7
	74.7	
C-25-16-15	85.3	86.8
	88.5	
C-30-16-6	30.5	30.0
	29.5	
C-30-16-8	38.8	39.4
	40.0	
C-30-16-10	49.9	48.5
	47.1	
C-30-16-12	73.6	74.7
	75.7	
C-30-16-15	85.1	88.3
	91.4	
C-35-16-6	33.2	31.9
	30.5	
C-35-16-8	40.5	42.7
	44.9	
C-35-16-10	53.3	51.8
	50.3	
C-35-16-12	79.1	78.2
	77.2	
C-35-16-15	88.1	89.3
	90.5	

(4) The ultimate pullout force of reinforced concrete is higher than that of plain concrete when the depth of embedded bars is shallow; when the embedded bars are deep, the type of concrete structure has little effect on the ultimate pullout force of embedded bars.

3. FINITE ELEMENT SIMULATION OF PLANTING BAR DRAWING AND FORMWORK SYSTEM

In this section, the finite element method is used for numerical analysis, and the Abaqus finite element model of the specimen is established, focusing on the constitutive relationship of the concrete base material, the reinforcement base material, and the parameter selection of the planting glue.

3.1 Establishment of planting bar drawing model

The ideal elastoplastic constitutive model is used for the reinforcement constitutive model. The concrete constitutive model uses the concrete plastic damage model (CDP model), and the damage performance of the concrete materials [26, 27] is described by the damage factor parameter. Tensile and compressive damage factor *dt* and *dc* are as follows:

$$d_t = \begin{cases} 1 - \sqrt{\rho_t[1.2 - 0.2x^5]} & (x \le 1) \\ 1 - \sqrt{\dfrac{\rho_t}{\alpha_t(x-1)^{1.7} + x}} & (x > 1) \end{cases}$$

$$d_c = \begin{cases} 1 - \sqrt{\dfrac{\rho_c n}{n - 1 + x^n}} & (x \le 1) \\ 1 - \sqrt{\dfrac{\rho_c}{\alpha_c(x-1)^2 + x}} & (x > 1) \end{cases}$$

Table 3. Plastic damage model parameters of C25 concrete

σ_c/MPa	ε_c^{in}/×10^{-3}	d_c	σ_t/MPa	ε_t^{ck}/×10^{-3}	d_t
13.306	0.000	0.000	2.129	0.000	0.000
19.028	0.766	0.314	2.026	0.022	0.126
17.496	1.445	0.450	1.847	0.053	0.254
14.988	2.159	0.553	1.605	0.085	0.365
12.748	2.862	0.629	1.399	0.116	0.451
10.955	3.550	0.684	1.235	0.146	0.517
9.543	4.223	0.726	1.106	0.174	0.569
8.425	4.885	0.759	0.919	0.229	0.645
7.526	5.539	0.784	0.697	0.332	0.735
6.473	6.509	0.814	0.489	0.530	0.821
5.338	7.946	0.847	0.209	1.680	0.933
4.217	10.077	0.878	0.084	6.235	0.978
2.865	14.786	0.917	0.052	12.271	0.988

Table 4. Plastic damage model parameters of C30 concrete

σ_c/MPa	ε_c^{in}/×10^{-3}	d_c	σ_t/MPa	ε_t^{ck}/×10^{-3}	d_t
15.969	0.000	0.000	2.390	0.000	0.000
22.835	0.754	0.290	2.274	0.025	0.132
21.137	1.332	0.411	2.027	0.059	0.267
18.175	1.952	0.512	1.709	0.095	0.386
15.435	2.565	0.590	1.453	0.128	0.476
13.207	3.160	0.649	1.259	0.160	0.543
11.447	3.739	0.695	1.111	0.191	0.596
10.053	4.305	0.730	0.903	0.248	0.670
8.936	4.862	0.759	0.669	0.357	0.757
7.636	5.684	0.792	0.458	0.567	0.838
6.244	6.898	0.828	0.191	1.790	0.940
4.887	8.691	0.864	0.120	3.409	0.966
2.773	14.796	0.921	0.075	6.635	0.981

Table 5. Plastic damage model parameters of C35 concrete

σ_c/MPa	ε_c^{in}/×10^{-3}	d_c	σ_t/MPa	ε_t^{ck}/×10^{-3}	d_t
18.631	0.000	0.000	2.629	0.000	0.000
26.641	0.695	0.257	2.502	0.026	0.129
23.678	1.375	0.403	1.947	0.096	0.373
19.120	2.105	0.525	1.682	0.131	0.460
15.414	2.809	0.613	1.315	0.196	0.579
12.687	3.480	0.676	1.083	0.257	0.654
10.685	4.128	0.723	0.815	0.371	0.743
9.184	4.759	0.758	0.374	1.021	0.892
7.120	5.990	0.808	0.152	3.566	0.963
4.866	8.389	0.865	0.095	6.941	0.979
2.584	14.806	0.925	0.060	13.655	0.988

Table 6. Other parameters of concrete plastic damage model

ψ	ε	f_{bo}/f_{co}	K	μ
30	0.1	1.16	0.6667	0.005

According to the formula, the relevant parameters of the plastic damage model of each numbered concrete were calculated, and the specific results were shown in Table 3, Table 4 and Table 5.

According to Abaqus modeling experience and convergence trial, other relevant parameters of plastic damage model of C25, C30 and C35 concrete are set in Table 6.

Establishment of planted bar pullout model: the concrete element and reinforcement element adopt the three-dimensional solid reduced integral element C3D8R type which can shorten the calculation time, and the concrete density is all set as 2,400kg/m^3; the simulation of planting bar glue is simplified as the viscous behavior in Abaqus. The stiffness and damage mode of rebar planting glue are simulated through the viscous behavior. The specific parameters are set according to the test results. The elastic modulus Knn of rebar planting glue is 2,700 MPa, and the shear modulus Kss and Ktt are set as 785 MPa. In the process of mesh generation for finite element modeling, the area with complex local stress at the interface between planted-bar reinforcement and concrete shall be densified.

3.2 Analysis results of the planted-bar drawing model

The simulation results of specimens are shown in Table 7.

According to the finite element simulation results of planted bar drawing, the ratio of the simulated maximum drawing force to the tested maximum drawing force is in the range of 0.89~1.07, which is more accurate for the simulation of the real drawing test, and the failure analysis conforms to the actual situation. The displacement of simulated reinforcement ends under the maximum drawing force is within the range of 0.84~1.33mm.

Table 7. Finite element simulation results of each specimen

No. of specimen	Ultimate pulling force simulation F_q/kN	The ultimate pulling force testing F_t/kN	F_q/F_t	The Displacement of the end of the steel bar under the simulated pole drawing force /mm
RC-30-12-6	19.5	19.1	1.02	1.15
RC-30-12-8	26.0	25.4	1.02	0.97
RC-30-12-10	32.1	30.7	1.05	1.10
RC-30-12-12	35.7	35.7	1.00	1.12
RC-30-12-15	41.4	40.8	1.01	1.32
RC-30-16-6	32.1	34.7	0.93	1.18
RC-30-16-8	44.6	43.7	1.02	0.84
RC-30-16-10	55.5	58.7	0.95	1.11
RC-30-16-12	77.9	77.1	1.01	1.17
RC-30-16-15	85.7	87.6	0.98	1.27
RC-30-20-6	55.9	58.8	0.95	1.21
RC-30-20-8	68.2	71.4	0.96	0.91
RC-30-20-10	88.3	94.3	0.94	1.22
RC-30-20-12	110.7	118.1	0.94	1.05
RC-30-20-15	133.4	135.1	0.99	1.28
C-25-16-6	27.2	25.7	1.06	1.02
C-25-16-8	37.9	36.2	1.05	1.00
C-25-16-10	48.2	46.1	1.05	1.09
C-25-16-12	65.0	72.7	0.89	1.13
C-25-16-15	86.5	86.8	1.00	1.32
C-30-16-6	29.3	30.0	0.98	1.22
C-30-16-8	42.5	39.4	1.08	0.98
C-30-16-10	51.3	48.5	1.06	1.06
C-30-16-12	69.3	74.7	0.93	1.24
C-30-16-15	87.8	88.3	0.99	1.27
C-35-16-6	31.1	31.9	0.97	1.11
C-35-16-8	45.7	42.7	1.07	1.03
C-35-16-10	53.4	51.8	1.03	1.21
C-35-16-12	72.4	78.2	0.93	1.12
C-35-16-15	88.6	89.3	0.99	1.33

3.3 Formwork system model

According to the provisions in Appendix A.0.4 of *Code for Construction of Concrete Structures* (GB50666-2011) [28], in order to make the checking calculation of formwork and planting bar parameters uniform and universal, the standard value of lateral pressure of newly poured concrete on formwork chooses the larger value in the above formula, i.e.

$$F = \gamma_c H$$

The steel plate adopts the three-dimensional solid reduced integration unit C3D8R, and the steel strength is defined by the parameters of Q235 steel in the specification. The influence of different construction parameters on the formwork engineering is discussed through finite element modeling. When meshing, the area with complex local stress at the interface between the steel formwork transverse rib and the fixed steel pipe is densified. The side pressure of concrete pouring is affected by the pouring height and has nothing to do with the pouring width, so the width of the established formwork is selected as 1m, the height is selected as 4m, the thickness of the steel panel is 4mm, the spacing between transverse ribs is 330mm, the spacing between longitudinal ribs is 250mm, and the height of ribs is 55mm. The formwork system has established the common Q235 steel panel, round steel pipe (Φ48×3.5) supporting components and butterfly fasteners models and overall model system.

The pressure load applied on the surface of the steel formwork is simulated, and the stress and deflection of the formwork system under 9 different working conditions (three different pouring heights: 2m, 3m, 4m and three different circular steel tube strut member spacing: 600 mm, 500 mm and 400 mm) during the concrete pouring process are analyzed, and calculation is made to check whether it meets the requirements.

Table 8. Maximum stress of steel formwork under different working conditions (unit: MPa)

Support interval (mm) / Casting height (m)	400	500	600
4	190	201	212
3	132	167	186
2	100	135	156

Table 9. Maximum displacement of steel formwork under different working conditions (unit: mm)

Support interval (mm) / Casting height (m)	400	500	600
4	1.49	1.79	2.32
3	1.25	1.54	2.11
2	0.98	1.21	1.55

The simulation results of all working conditions are summarized in Table 8 and Table 9.

Taking the one with an height of 4m and the spacing between round steel tubular supports 600mm as an example, the maximum pouring load under this working condition is $\gamma_c H$=25kN/m^3×4m=100kN/m^2/. The supports are placed at the most unfavorable position of the steel formwork according to the transverse spacing of 600mm, and the connectors are placed according to the spacing of 1,000mm. The maximum stress of the formwork and supports is calculated to be 212MPa (as shown in Figure 1), which is less than the design value 215MPa of tensile strength of Q235 steel. The strength meets the requirements, and the maximum displacement of the formwork is 2.32mm (as shown in Figure 2). It is larger than the allowable deflection of steel formwork panel specified in 4.4.2 of the *Technical Code for Composite Steel Formwork* (GBT50,214-2013) [29], and the rigidity does not meet the requirements.

It can be seen from Table 8 that all working conditions with pouring heights of 2m, 3m and 4m meet the requirements that the steel formwork stress is less than the design value of Q235 steel tensile strength. It can be seen from Table 9 that there are four working conditions that meet the formwork displacement limit for concrete pouring: the building height is 4m, and the interval between round steel tubular supports is 400mm; the building height is 3m, and the spacing between round steel tubular supports is 400mm; the building height is 2m, and the spacing between round steel tubular supports is 400mm; the building height is 2m, and the spacing between round steel tubular supports is 500mm.

It can be seen from the above results that the building height 4m, and the spacing of round steel tubular supports 400mm meet the requirements of the specification for the strength and stiffness of steel formwork. Therefore, the spacing of planting bars is selected according to the horizontal spacing 400mm and the vertical spacing 1,000mm. At this time, the maximum pulling force of the planting bar system is 34.8kN. In view of the influence of factors such as the difference in the performance of different planting glue, the difference in the construction environment, and the difference in the operating level of the construction personnel, 20% safety reserve is considered for the selection of the diameter and depth of the planted-bar reinforcement, that is, the pulling force of the planted rebar should not be less than 1.2 times the maximum pulling force obtained from the test, that is, the pulling force of the planted rebar should not be less than 41.8kN. According to the pull-out test and finite element simulation results, the diameter of planted bar can choose to be Φ16 and above, and the depth of planted bar shall not be less than 8d or the diameter of planted bar can choose to be Φ20 and above, and the depth of planted bar shall not be less than 6d.

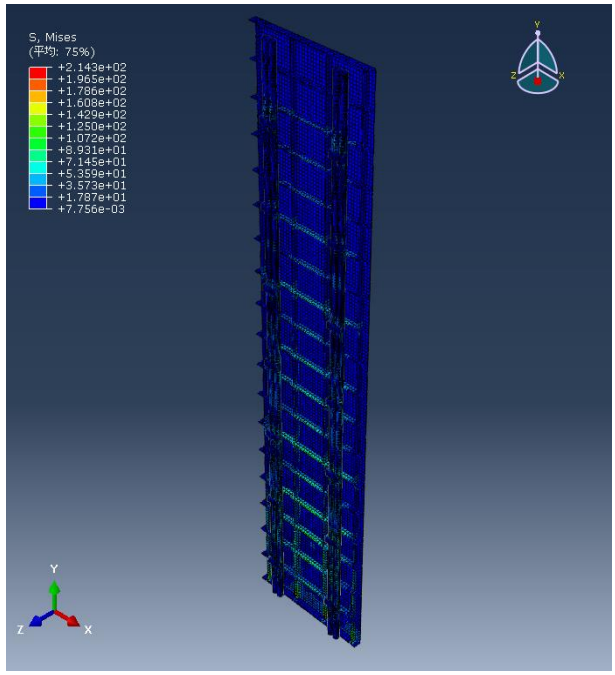

Figure 1. Stress nephogram of steel panel and steel pipe support under working condition 1 (unit: MPa)

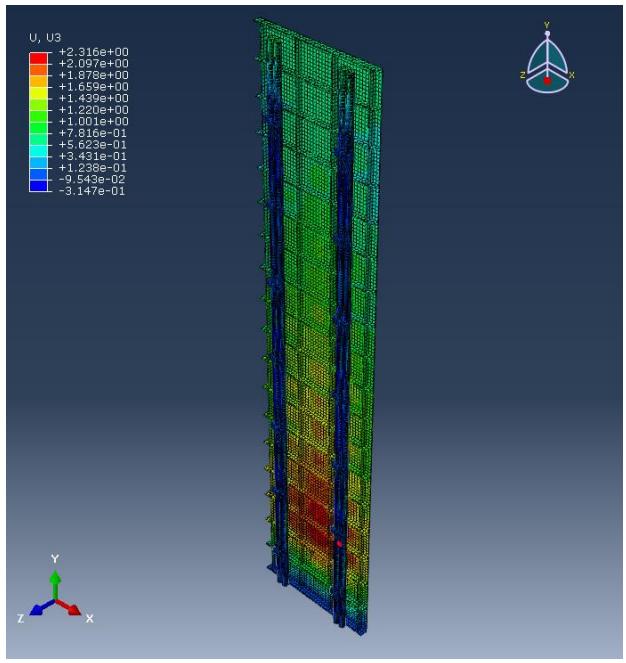

Figure 2. Displacement nebulae of steel panel and steel pipe support under working condition (Unit: mm)

Under various requirements, the remaining three working conditions meeting the stiffness shall be adjusted:

Working condition 1: the building height is 3m and the spacing between round steel tubular supports is 400mm; the maximum pulling force of planted reinforcement is 25.2kN and the pulling force of the planted reinforcement after considering the safety reserve is no small than 30.2kN. Under this condition, the steel reinforcement with the diameter of

Φ12 or above and with the depth not less than 12d or with the diameter of Φ16 or above and with the depth not less than 6d can be chosen. Working condition 2: the building height is 2m and the spacing between round steel tubular supports is 400mm; the maximum pulling force of planted reinforcement is 10.0kN and the pulling force of the planted reinforcement after considering the safety reserve is not smaller than 12.0kN. Under this condition, the steel reinforcement with the diameter of Φ12 or above and with the depth not less than 6d can be chosen. Working condition 3: the building height is 2m and the spacing between round steel tubular supports is 500mm; the maximum pulling force of planted reinforcement is 12.5kN and the pulling force of the planted reinforcement after considering the safety reserve is not smaller than 15.0kN. Under this condition, the steel reinforcement with the diameter of Φ12 or above and with the depth not less than 6d can be chosen.

4. CONCLUSION

Selection of appropriate planted bar parameters for different construction conditions:

(1) When the pouring height is 4m, the spacing between round steel tubular supports should be 400mm, and the spacing between longitudinal connectors can be 1,000mm. After considering 20% of the safety reserve, the steel reinforcement with the diameter of Φ16 or above and with the depth not less than 8d or with the diameter of Φ20 or above and with the depth not less than 6d can be chosen.

(2) When the pouring height is 3m, the spacing between round steel tubular supports shall be 400mm, and the spacing between longitudinal connectors can be 1,000mm; After considering 20% of safety reserve, the steel reinforcement with the diameter of Φ12 or above and with the depth not less than 12d or with the diameter of Φ16 or above and with the depth not less than 6d can be chosen.

(3) When the pouring height is 2m, the spacing between round steel tubular supports shall be 500mm, and the spacing between longitudinal connectors can be 1,000mm; After considering 20% of safety reserve, the steel reinforcement with the diameter of Φ12 or above and with the depth not less than 6d can be chosen.

REFERENCES

[1] Høien, A.H., Nilsen, B., Olsson, R. (2019). Main aspects of deformation and rock support in Norwegian road tunnels. Tunnelling and Underground Space Technology, 86: 262-278. https://doi.org/10.1016/j.tust.2019.01.026

[2] Zhang, X., Yang, Y., Yang, Z., Zheng, Y. (2020). Construction method of port building structure joint reinforcement of port building structure. Journal of Coastal Research, 103(SI): 422-425. https://doi.org/10.2112/SI103-086.1

[3] Liu, Y., Yin, S., Wu, Y., Zhao, Y. (2017). The raft foundation reinforcement construction technology of Hongyun Building B tower. In IOP Conference Series: Earth and Environmental Science, 81(1): 012124. https://doi.org/10.1088/1755-1315/81/1/012124

[4] Lee, J.C. (2020). Analysis of the rebar quantity take-off according to the application of seismic reinforcement details for RC apartments. Journal of the Architectural Institute of Korea, 36(9): 167-174. https://doi.org/10.5659/JAIK.2020.36.9.167

[5] Bronevizky, A.P. (2017). Temporary reinforcement of structures for building reconstruction. Science & Technique, 16(2): 137-143. https://doi.org/10.21122/2227-1031-2017-16-2-137-143

[6] Blikharskyy, Y., Khmil, R., Blikharskyy, Z. (2018). Research of RC columns strengthened by carbon FRP under loading. In Matec Web of Conferences, EDP Sciences, 174: 4017. https://doi.org/10.1051/matecconf/201817404017

[7] Vanagas, E., Kliukas, R., Lukoševičienė, O. (2017). Strength of circular concrete columns reinforced with FRP bars and spirals. Procedia Engineering, 172: 1220-1226. https://doi.org/10.1016/j.proeng.2017.02.143

[8] Hack, N., Bahar, M., Hühne, C., Lopez, W., Gantner, S., Khader, N., Rothe, T. (2021). Development of a robot-based multi-directional dynamic fiber winding process for additive manufacturing using shotcrete 3D printing. Fibers, 9(6): 39. https://doi.org/10.3390/fib9060039

[9] Dzhamuev, B. (2018). Using of carbon fiber fabric for reinforcement the walls of the aerated concrete blocks in buildings, constructed in seismic regions. In MATEC Web of Conferences, 251: 02041. https://doi.org/10.1051/matecconf/201825102041

[10] Ferreira, D., Bairán, J.M., Marí, A. (2016). Shear strengthening of reinforced concrete beams by means of vertical prestressed reinforcement. Structure and Infrastructure Engineering, 12(3): 394-410. https://doi.org/10.1080/15732479.2015.1019893

[11] Ajith, K., Mathew, A. (2019). Experimental and analytical study on strengthening of reinforced concrete t-beams using external prestressing. In National Conference on Structural Engineering and Construction Management, 46: 465-474. https://doi.org/10.1007/978-3-030-26365-2_43

[12] El-Hacha, R., Awassa, O. (2021). Strengthening of concrete structures using prestressed FRP–A review. In International Conference on Fibre-Reinforced Polymer (FRP) Composites in Civil Engineering, 198, pp. 2209-2221. https://doi.org/10.1007/978-3-030-88166-5_191

[13] Zhu, G. (2020). Application of comprehensive method in strengthening of a tall building. In IOP Conference Series: Earth and Environmental Science, 446(5): 052108. https://doi.org/10.1088/1755-1315/446/5/052108

[14] Moffat, R., Jadue, C., Beltran, J.F., Herrera, R. (2017). Experimental evaluation of geosynthetics as reinforcement for shotcrete. Geotextiles and Geomembranes, 45(3): 161-168. https://doi.org/10.1016/j.geotexmem.2017.01.007

[15] Massone, L.M., Nazar, F. (2018). Analytical and experimental evaluation of the use of fibers as partial reinforcement in shotcrete for tunnels in Chile. Tunnelling and Underground Space Technology, 77: 13-25. https://doi.org/10.1016/j.tust.2018.03.027

[16] Lin, A., Ostertag, C.P. (2021). Interaction between high performance fiber reinforced cement-based composites and steel reinforcement. Engineering Structures, 247: 113173. https://doi.org/10.1016/j.engstruct.2021.113173

[17] Beliaev, M., Semenov, A., Semenov, S., Benin, A. (2016). Simulation of pulling the reinforcing bar from concrete block with account of friction and concrete damage. In MATEC Web of Conferences, 73: 4010. https://doi.org/10.1051/matecconf/20167304010

[18] Lin, A., Ostertag, C.P. (2017). Multi-scale pull-out resistance of steel reinforcing bar embedded in hybrid fiber reinforced concrete (HyFRC). In IOP Conference Series: Materials Science and Engineering, 246(1): 012022. https://doi.org/10.1088/1757-899X/246/1/012022

[19] Wardeh, G., Ghorbel, E., Gomart, H., Fiorio, B. (2017). Experimental and analytical study of bond behavior between recycled aggregate concrete and steel bars using a pullout test. Structural Concrete, 18(5): 811-825. https://doi.org/10.1002/suco.201600155

[20] Qasem, A., Sallam, Y.S., Eldien, H.H., Ahangarn, B.H. (2020). Bond-slip behavior between ultra-high-performance concrete and carbon fiber reinforced polymer bars using a pull-out test and numerical modelling. Construction and Building Materials, 260: 119857. https://doi.org/10.1016/j.conbuildmat.2020.119857

[21] Tierney, L., Safiuddin, M. (2022). Insights into Concrete Forming, Reinforcing, and Pouring in Building Construction. Buildings, 12(9): 1303. https://doi.org/10.3390/buildings12091303

[22] Henschen, J.D., Castaneda, D.I., Lange, D.A. (2018). Formwork pressure model for self-consolidating concrete using pressure decay signature. ACI Materials Journal, 115(3): 339-348. https://doi.org/10.14359/51702183

[23] Teixeira, S., Santilli, A., Puente, I. (2016). Analysis of casting rate for the validation of models developed to predict the maximum lateral pressure exerted by self-compacting concrete on vertical formwork. Journal of Building Engineering, 6: 215-224. https://doi.org/10.1016/j.jobe.2016.03.008

[24] Haidar, H.H., Mussa, F.I., Dawood, A.O., Ghazi, A. A., Gabbar, R.A. (2020). Experimental study of post installed rebar anchor systems for concrete structure. Civil and Environmental Engineering, 16(2): 308-319. https://doi.org/10.2478/cee-2020-0031

[25] Ding, W., Leng, F.G., Wei, Q.D., Zhang, X.F., Zhou, Y.X., Tian, G.F., He, G.X., Ji, X.K., Wang, J. (2011). Code for design of common concrete mix (JGJ55-2011). Concrete World, 2011(12): 76-79.

[26] Yadav, I.N., Thapa, K.B. (2020). Fatigue damage model of concrete materials. Theoretical and Applied Fracture Mechanics, 108: 102578. https://doi.org/10.1016/j.tafmec.2020.102578

[27] Baraka, A., Matallah, M., Djafour, M., Bouazza, M. (2018). Caractérisation des effets régissant le comportement dynamique du béton. Matériaux & Techniques, 106(5): 502. https://doi.org/10.1051/mattech/2018043

[28] Guo, Z.X., Wang, Y.L., Jiang, B. (2012). Code for construction of concrete structures, GB50666-2011. Technique of Construction, 2012, 41(3): 5-10.

[29] Mi, J.P. (2014). Technical specification for composite steel formwork, GB/T50214-2013. Technique of Construction, 2014 (5): 21-23.